6-2012

Neural Responses to Looming Objects in the Dragonfly

Elon Gaffin-Cahn
Union College - Schenectady, NY

NEURAL RESPONSES TO LOOMING OBJECTS IN THE DRAGONFLY

By

Elon Gaffin-Cahn

****

Submitted in partial fulfillment of the requirements for Honors in the Department of Biological Sciences

UNION COLLEGE

June 2012

ABSTRACT

GAFFIN-CAHN, ELON Neural Responses to Looming Objects in the Dragonfly. Department of Biological Sciences, June 2012.

ADVISOR: Robert M. Olberg

Dragonflies have high visual acuity, which, when combined with a remarkably fast visual response, allows them to hunt small insects with a high success rate. Rather than aiming at the prey's current location, the dragonfly predicts the prey's future location and intercepts the insect mid-flight. Eight bilateral pairs of large Target-Selective Descending Neurons (TSDNs) of the dragonfly ventral nerve cord respond to small, contrasting objects, which presumably represent potential prey. These interneurons are part of the neuronal circuitry that triggers small changes in wing angle and position to control flight during prey interception. In flight, dragonflies extend their legs out to catch the prey about 20 ms before contact. The current research investigates the role of the TSDNs in prey contact. Spiking traces from the nerve cord were recorded during the presentation of expanding black circles projected on a screen, which simulate approaching prey. Several loom sizes and speeds were used to cover a range of realistic and unrealistic rates of expansion. I hypothesized that the interneurons predict the time to contact (Tc) of the simulated looming stimuli. Looming-sensitive TSDNs fired at a consistent time before Tc, supporting the hypothesis.

Acknowledgements

I would like to thank my thesis advisor, teacher, and mentor, Robert M. Olberg for his unwavering support and provider of insight. Helping me through several months of failed attempts at data collection, he has been an amazing inspiration and has taught me everything I know about dragonflies, neurobiology, neuroethology, and how to bring enthusiasm and fun into the lab setting.

I thank the Air Force Office of Scientific Research for funding my summer research fellowship and for supporting my attendance of the East Coast Nerve Net conference. I would also like to thank the Union College Department of Biological Sciences and the Undergraduate Research Fund for funding my trip to San Diego for the Experimental Biology conference.

Table of Contents

Table of Figures

Introduction

Dragonflies earned themselves the nickname "devil's darning needles" because of their apparent danger as menacing fliers (Needham et al. 2000). However, this could not be farther from the truth, at least from a human perspective. Defending our own species from pests such as mosquitoes and gnats, dragonflies patrol the skies with speed, agility, and grace. The roughly 350 North American species (Needham et al. 2000) fill a massive niche that displays a wide variety of colors and sizes, but are all skilled fliers.

Dragonflies belong to the order Odonata, and represent the suborder Anisoptera (Nikula et al. 2003). Modern Odonata, which also includes Zygoptera, the damselflies, date back 145 to 210 million years ago, along with the emergence of dinosaurs, although the Odonata's close predecessors can be traced to before 335 million years ago (Silsby 2001). Their highly conserved structure, as evidenced by fossil records, is a testament to their prowess. They are phenomenal predators in flight, aided by their visual system. For example, the compound eye of some large Aeshnid family dragonflies contains over 28,000 ommatidia (Sherk 1978), and dragonflies can see nearly 360˚ around them (Corbet 1999). Prey capture success rates have been reported in species *Pachydiplax longipennis* as low as 65% (Baird and May 1997) and as high as 97% for *Erythemis simplicicollis* and *Leucorrhinia intacta* (Olberg et al. 2000). In both studies, these values were determined based on observation of post-capture mastication. In addition, all three species analyzed are in the family Libellulidae, which were used in the current study.

Although dragonflies are known for their spectacular ability to catch prey, they are also the subjects of predation. The most dangerous to them are amphibians, reptiles, and birds, although there are accounts of dragonflies being eaten by mammals, other

insects, a New Zealand trout, and carnivorous plants (Corbet 1999). The size of this list and frequency of predation on dragonflies gives the false impression that they are easy targets. Corbet (1999) warns against coming to this conclusion by including in his discussion that the dragonflies are most vulnerable as tenerals, during mating and oviposition, and when flying in large aggregates. He admits that cruising adult Anisoptera are masters of evasion, with the exception of only a few cases of predation.

On the other side of the food chain, dragonflies typically prey on small insects, the size of which depends on the species and size of predator. True flies, of order Diptera, provide over 75% of foraged prey for *Pachydiplax longipennis* (Baird and May 1997). Of all their consumed prey items, over 50% were between 1 and 2 mm long, while other size prey were infrequently captured. In a study using beads on a fine wire to simulate artificial prey items, Olberg et al. (2005) found that nearly 80% of *Sympetrum vicinum* foraging flights were attempts to capture fake prey of size 1.5 to 3 mm. It is important to note that *Pachydiplax* and *Sympetrum* are relatively similar in size because species size affects prey size. This study also included foraging flights of a slightly larger dragonfly in the family Libellulidae, *Libellula luctuosa*, which were recorded to be 42 to 50 mm in length (compared with *Sympetrum's* length of 31-35 mm). It follows that a larger species would hunt larger prey, and this is exactly what Olberg and colleagues found. Over 80% of *Libellula* prey capture flights were for glass beads between 1.8 and 5 mm in diameter.

Dragonfly flight speeds can also vary based on size, species, and reason for flight - predation, escape, territory defense, mating, or simple cruising behavior. Rüppell (1989) studied many species of Odonata, including several in the family Libellulidae. Of those Libellulid species whose flight speed was measured, top speeds ranged from 4.0 to 4.3

m/s. Other Libellulid species have been reported as having top speeds as low as 2.6 m/s and as high as 4.0 m/s (Wakeling and Ellington 1997). Flight speed during prey capture, however, will be much slower than these recorded velocities. Raw, unpublished high-speed videos of prey or simulated prey capture show that Libellulidae fly at 0.5 to 1.0 m/s during their pursuit. Their prey capture flights are so short, that they are still accelerating to full speed when they catch their prey (Leonardo, unpublished).

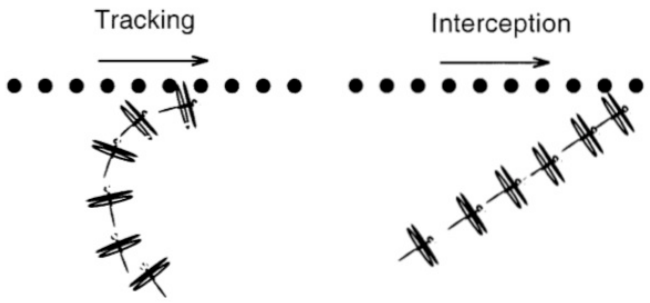

Figure 1. **Two types of predation behavior: tracking and interception.** Dragonflies perform interception shown on the right side of the figure. This behavior does not require being faster than their prey, but makes capture substantially easier. Figure reproduced with permission from Olberg et al. (2000).

Predatory behavior, or any collision course, whether on land, in the water, or in the sky, can be classified into two types: tracking and interception (Collett and Land 1978; Olberg et al. 2000). The process of tracking involves the predator aiming toward the prey's current location. If the predator is faster than the prey and the prey is moving in a straight line, then the predator's motion will be curved and the two animals will slowly converge. Tracking is therefore relatively straightforward behavior for a nervous system to carry out. In contrast, the process of interception is a complex behavior that involves the prediction of the prey's future location. To do this, the predator must have information about the prey's angular velocity and either distance or speed. The pursuer will keep the prey at a constant angle in its field of view, and move in a straight line such that their two paths will intersect. This behavior does not require the predator to be faster, but if it is not, then it will require other biologically stealthy skills. In the dragonfly's

case, it will nearly always be faster than its prey. Dragonflies, despite their small size and relatively simple nervous system, are able to carry out the complex behavior of interception (Olberg et al. 2000). Figure 1 shows a visualization of the two methods of predation. As I described, for a straight-moving prey, a tracking predator will move in a curved fashion, whereas an intercepting predator is able to move in a straight line, keeping its prey at a constant bearing.

The cross section of the dragonfly ventral nerve cord, which descends from the brain to the thorax and abdomen, reveals several startlingly large axons. They are reminiscent of the locust descending contralateral movement detector (DCMD), which has been reported to play a role in the collision-avoidance mechanism (Gray et al. 2001; Santer et al. 2006). The locust's collision-avoidance mechanism is important for evasion of both abiotic yet potentially harmful objects, as well as purposefully injurious predators. In many animals, escape behaviors are controlled by large axons because the signal will travel down a large axon faster than a small axon. Therefore, it is expected that this neuronal makeup has a similar role in the dragonfly. However, this is not necessarily the case. Unlike the large axons of the locust, those of the dragonfly may have evolved for confrontation, not avoidance.

The giant axons of the dragonfly nerve cord are named the target-selective descending neurons (TSDNs) based on their anatomy and their discriminatory response to small, contrasting objects (Olberg 1986). As can be seen in Figure 2, near the dorsal edge of the two connectives of the ventral nerve cord, there are eight bilateral pairs of TSDNs, all of which play a role in target response. Some Aeshnid family TSDNs are up to a 30 or 40 μm in diameter, making them a sizeable fraction of their 450 μm nerve cord

(Olberg 1986). Unpublished observations of Libellulid dragonflies, which are typically smaller than the Aeshnidae, have shown that while the nerve cords are proportionally smaller, the Libellulid TSDNs are comparable in size to those in the Aeshnidae, further suggesting the importance of their fast conduction speed.

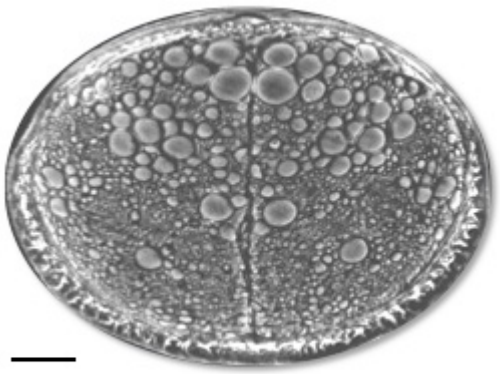

Figure 2. **Cross-section of Aeshnid ventral nerve cord.** Hundreds of axons can be seen, but the TSDNs are the massive ones, which tend to lie on the dorsal (top) side. Scale bar is 50 μm. Figure reproduced with permission from Olberg (1986).

If a neuron has fast conduction speed, it likely has evolutionarily important circuitry downstream. Olberg (1983) showed that 200 Hz intracellular stimulation elicited a downstream wing flapping behavior. While it was only the stimulation of MDT1 that created an extreme behavior, the subtler wing angle shifts triggered by stimulation of the other TSDNs are interpreted as steering movements, which is critical in both prey pursuit and collision avoidance. However, it is not clear exactly how stimulation of which combination of TSDNs will create the wide variety of different wing flapping and angle change behaviors.

What elicit an initial response from the TSDNs are small, contrasting, moving objects. However, this analysis alone is insufficient. Each of the eight interneurons responds to a preferred direction of motion (Olberg 1986; Frye and Olberg 1995). Each TSDN does not fire for one precise direction, but rather fires during motion in a range of directions about 60º wide. This broad directional tuning is certainly a benefit, however, because it allows for overlapping receptive fields, so that any given direction of motion will induce a unique pattern of TSDN spikes.

Olberg (1986) and Frye and Olberg (1995) found that despite the strong directional selectivity of most of the TSDNs, two of them, DIT3 and MDT3, respond to the anti-preferred direction as well. This finding suggests that these neurons have a special role in dragonfly flight. Through unpublished observations, we have noticed that these two neurons respond to looming objects. A looming stimulus is any object which approaches the observer, which in this case is the dragonfly. The looming stimulus can be approaching for any reason - predation, prey capture, or abiotic factors. Regarding prey capture, I will define a looming stimulus to include a prey moving away from the dragonfly, as long as the distance between them is decreasing. If the net distance between predator and prey is decreasing, the angle subtended on the predator's retina by the prey is increasing.

Keeping the prey at a constant bearing to its flight direction, the dragonfly holds the target directly on the fovea. As the time to interception gets closer, the prey will subtend an increasingly large angle on the dragonfly's visual field. This increase in angle, and its derivative – the rate of expansion – can be can be quantified if the speed of approach and the size of the prey are known. Using fundamental algebra and trigonometry, Gabbiani et al. (1999) show that the rates of expansion of two different stimuli are equivalent as long as the ratio of the half-size l (for practical matters, the radius) of the approaching object to the speed of approach v is held constant. The rate of expansion then, is dependent on the value of this variable ratio l/v. Because l/v is a ratio of size to speed, it is measured in units of time, which are typically seconds.

Gabbiani et al. (1999) varied the l and v of looming black squares projected onto a screen to test the optimal response of the locust DCMD. They observed that the DCMD

had a baseline firing rate below 1 Hz, and that depending on the *l/v* value of the looming stimuli, the firing rate would increase dramatically. The greatest average number of spikes elicited over several trials was 23, which corresponded to an *l/v* = 0.045 s. They calculated spike frequencies and the distribution of spikes over each trial, which allowed them to determine which *l/v* stimulus would best be able to predict the peak firing rate. For example, despite that the loom with *l/v* = 0.045 s produced the greatest average number of spikes per trial, its distribution of spikes was wide, and therefore its spike frequency was not sharp. Generally, the greater the *l/v* value the stimulus, the less temporal resolution of time before contact. Time to contact (Tc) was defined as the moment the object would hit the animal, or, in the case of 2D projected stimuli; the moment the stimulus was calculated to "hit" the animal. In the case of prey pursuit, Tc is the moment of capture.

When recording from the DCMD and the TSDNs in their respective animals, one important difference becomes immediately clear, even before presentation of any stimulus. As I mentioned, the DCMD has a baseline firing rate just below 1 Hz. The TSDNs, however, are completely silent until the animal is presented with an appropriate stimulus. Only a stimulus to which they respond will induce any firing at all. Moreover, as I will discuss in greater depth, the presentation of a relevant looming stimulus will elicit far fewer spikes in the TSDNs than the DCMD. This limits the ability to gather spike frequency information, but we can use the spiketimes themselves instead of a mathematically-calculated instantaneous frequency. While instantaneous frequency is the relevant statistic for DCMD analysis, spiketimes, the moments during an electrical recording that a neuron fires, are used for the TSDNs.

Both the DCMD and the TSDNs are movement detectors which are part of circuitry that controls their respective animals' own physical response. But, another fundamental difference is their biological role in this motive response, as shown in the model in Figure 3.

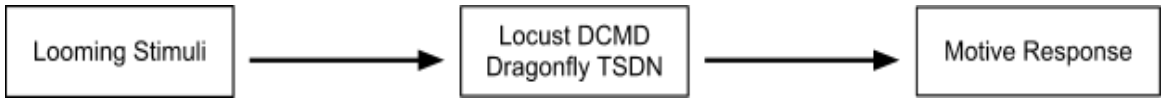

Figure 3. **Neural model of the DCMD and TSDNs.** Looming targets approach the locust or the dragonfly, which elicits a response from the DCMD and the two looming-sensitive TSDNs, respectively. The DCMD and TSDNs are upstream of circuitry that controls a motive response, but the manner in which they do this is still unknown. In addition, the type of motive response, avoidance or approach, may be different in the two situations.

Research has shown that the DCMD has a role in collision avoidance (Gabbiani et al. 1999; Gray et al. 2001; Santer et al. 2006), but the equivalent role of TSDNs is not as well understood. It is feasible that the looming-sensitive TSDNs are involved in prey pursuit, which would in essence have the opposite role of collision-avoidance mechanisms of the DCMD. But, they may also play a role in predator and abiotic factor evasion. Their role will not be understood until we know exactly how each TSDN effects flight.

Whether foraging for prey or evading approaching objects, flight maneuvers must be carried out quickly and with precision. During predation, dragonflies exhibit behavioral patterns that are highly conserved between individuals. Before takeoff, the dragonfly will center the prey within 3º on the intersection of its visual midline and its dorsal foveal band, which runs left-right on the dorsal side of the eye (Olberg et al. 2007). In addition, analysis of high-speed video footage showed that dragonflies consistently release their legs about 20 ms before prey capture (Worthington, unpublished).

Previous research has shown that the TSDNs have downstream effects on wing muscles Olberg (1983), and there is evidence that dragonflies exhibit consistently timed behavior prior to prey capture. Therefore, it is possible that the TSDNs have a role in these consistently timed behaviors. For this to be true, TSDNs would necessarily have two properties. First, they would need to be upstream of muscle circuitry which controls the behavior, for which there is evidence. Second, the timing of the TSDN firing pattern would have to be consistent before the temporally predictable behavior, which is the current focus.

In the present study, I investigated whether the looming-sensitive TSDNs can predict the time to interception of the prey item. I tested this by generating a simulated looming object, which represents the prey, on a screen in front of the dragonfly. I hypothesize that those looming-sensitive TSDNs can predict time to contact (Tc) within a realistic range of values of *l/v*, values that the dragonfly would normally encounter as prey in nature. This would allow the dragonfly to make any last-moment adjustments to the flight path, and to prepare the legs for stretching out to catch the prey. The TSDNs should fire at a consistent interval before simulated Tc. Simulated Tc can be calculated from the rate of expansion, which is based on the *l/v* value of the looming stimulus.

Methods

Subjects

Recordings were performed on species *Libellula pulchella* (n = 10), the Twelve-Spotted Skimmer, of the Libellulid family. During the colder months when the experiment was performed, adult dragonflies had migrated to warmer climates, so animals whose data were included in this study were caught as diapausing larvae in

Niskayuna, NY. They were then stored in the dark at 4˚C. Each week, a group of larvae was replaced into room temperature water, fed black worms (*Lumbriculus variegates*) and emerged from their exuviae at their own pace. Once they emerged and their wings were fully spread, they were placed in a dark, room temperature container for one day, and then a 4˚C refrigerator until they were needed. Their lifespan in the cold would expire around 7 to 10 days, so they were used as promptly as possible after emergence. As adults after emergence, they were not fed because they do not forage in restricted indoor flight cages (Olberg et al. 2007).

Physical Setup

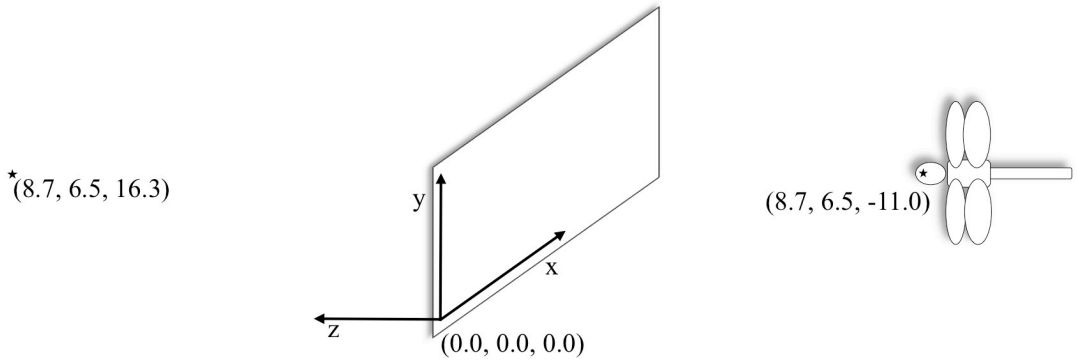

Figure 4. **Spatial set-up.** The coordinate system used is based on the projected image, such that the origin is located at the bottom left-hand corner of the screen. Stimuli were projected onto the screen from the positive z direction. The looming stimuli, as discussed below, simulates prey moving from the left star at (8.7, 6.5, 16.3) in the negative z direction, through the screen at z = 0, to the right star at the dragonfly's fovea at (8.7, 6.5, -11). These coordinates are measured in centimeters, and the x-, y-, and z-axes are not drawn to scale with each other.

Dragonflies were mounted stationary to a metal rod using a mixture of 50% beeswax and 50% resin, which have a low melting temperature when combined. This both avoids harming the dragonfly and increases ease of preparation. The animals were fixed ventral-side up with the head also held stationary so that the intersection of the dorsal foveal band and the visual midline was aimed directly at the center of the screen. The fovea was kept 11.0 cm from the center of the screen, such that where the center of

the screen has coordinates (8.7, 6.5, 0.0 cm), the eyes had coordinates (8.7, 6.5, -11.0 cm), as shown in Figure 4. These ostensibly arbitrary coordinates derive from the program used to run stimuli and the distance from the projector to the screen.

A ThorLabs DET110 photodiode, run through a window discriminator, triggered recording at the stimulus onset to ensure precise timing when matching the stimulus with the electrical trace, which was recorded with an A-M Systems Differential AC Amplifier Model 1700 and digitized with ADInstruments PowerLab 4/25. Electrical traces from the recording wire and photodiode were displayed and recorded with LabChart software (ADInstruments). I used a broken glass microelectrode to record from the TSDNs of interest. In addition, I inserted a silver wire body ground into the subject's thorax or abdomen. All nearby electronic equipment was grounded. This method was sufficient enough to afford a satisfactory signal-to-noise ratio. Spike traces were analyzed with DataView software, which sorts a trace into individual spiketimes for each unit being recorded.

Stimuli

I presented stimuli to the dragonflies from a 360 Hz InFocus DepthQ projector. Such high refresh frequency is required because of dragonflies' remarkable fast flicker fusion frequency (fff) - the refresh time of the visual system. The dragonfly fff can be as fast as 220 Hz, but is typically between 100 Hz to 200 Hz (Ruck 1961). Previous experiments have used rates of 200 Hz in their presentation of stimuli (Geurten et al. 2007; Wiederman and O'Carroll 2011).

Scripts were written using the software Stimulate OpenGL developed by Calin Culianu and Anthony Leonardo and were used to generate the scanning stimulus and the

simulated looming objects. A scanning stimulus, or simply 'scan', is a stimulus that moves with constant size at a constant speed across the screen. TSDNs respond directionally, so the scan was used as a preliminary data set to determine which TSDN was being recorded during the looming stimuli. The program was run on Windows XP and connected to the projector, which flashed on an 800x600 pixel screen. The scan consisted of eight directional paths established by vectors written in the script. Each path had an x and y component, one of which was dominant, such that the paths moved at approximately 3º, 86º, 94º, 177º, 183º, 266º, 274º and 357º relative to the horizontal, positive-x direction. The speed in the dominant direction was held constant but the secondary direction speed was different if the scan moved in the x or the y direction so that each path would be exactly 15 seconds on the rectangular (non-square) screen. Figure 5 is an example of the time course of a scan whose dominant direction is positive x (rightward) and whose secondary direction is positive y (upward).

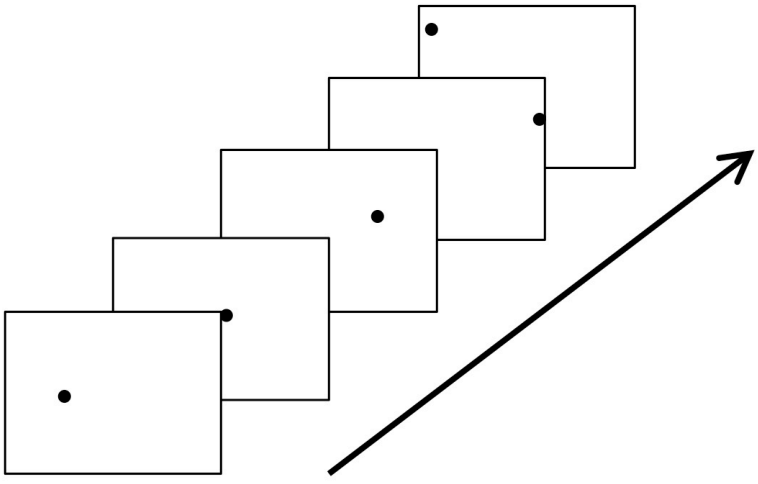

Figure 5. **Time course of a scanning object.** This figure contains five snapshots in a scanning stimulus. As time progresses, represented by the direction of the arrow, the stimulus is dominated by positive-x (rightward) motion and has a secondary motion in the positive-y (upward) direction. At a refresh rate of 360 Hz, each full scan was composed by 5400 frames and took 15 seconds. When the scan moves off the screen, it wraps back on the opposite side, as shown in the fifth snapshot. The stimuli are not drawn to scale, nor does the time elapsed relate accurately to the position of the stimuli.

An object's motion toward the dragonfly was simulated by a growing black circle projected on the screen. Looming stimuli were recorded for 2605 ms, 100 ms longer than the slowest loom presented. Inter-stimulus intervals were 45 seconds long between each of the 15 looming stimuli to prevent any chance of TSDN habituation. Five values of *l* (0.022, 0.043, 0.086, 0.173, 0.346 cm) and three values of *v* (10.81, 43.22, 172.89 cm/second) were used such that values of *l/v* doubled from 0.00025 s to 0.064 s, a 16-fold increase and decrease of the realistic value, *l/v* = 0.002 s, which was flashed three times.

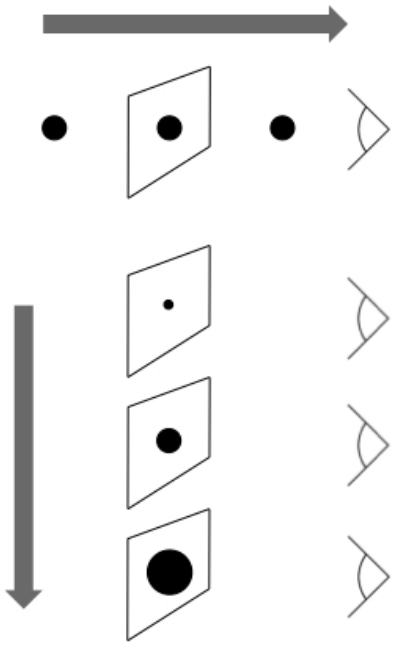

Figure 6. **Time course of a looming object.** The top section represents the simulated approaching object, the condition found in nature. It remains the same size over time, but imposes a larger percent of the eye's field of view because of its approach. Below, the projected loom does not change in distance from the viewer, so it increases in size to simulate the increasing angle subtended on the eye in the top section of the figure. The looming objects are not drawn to scale, nor do the three stages depicted correlate to a real size of expansion (*l/v*) used in the experiment.

Looming stimuli simulated a starting location at (8.7, 6.5, 16.3 cm), simulated traveling through the screen and ended at (8.7, 6.5, -10.8 cm), which subtended a large portion of the dragonfly's visual field. Figure 6 shows what the projected loom simulates. The software outputs a growing circle that simulates an approaching object. Conceptually, what is being simulated is a loom that does not grow in size, just as a dragonfly's prey would not change size. But, as the distance from the dragonfly to the prey decreases, so the angle that the object subtends on the dragonfly's retina increases. The projected loom does not change distance from the eye, so to compensate, it must increase in size in order to imitate the increasing subtending angle, as shown in Figure 6. Figure 7 shows the breakdown of the *l/v* values for the

looming stimuli. The three approach speeds and five stimulus sizes divide out to 15 *l/v* values, nine of which are discrete.

		l/v (s)		
		v (cm/s)		
		10.81	43.22	172.89
	0.022	**0.002**	0.0005	0.000125
	0.043	0.004	0.001	0.00025
l (cm)	0.086	0.008	**0.002**	0.0005
	0.172	0.016	0.004	0.001
	0.346	0.032	0.008	**0.002**

Figure 7. **Breakdown of *l/v* values.** These are the nine discrete *l/v* values used in the looming stimuli, where the realistic *l/v* values are in bold. Note that these values of *l* are not the stimulus sizes – they are the half-sizes, or radii. The actual stimulus sizes used in the parameters of the stimulus generation program were double these values.

Results

All ten *Libellula pulchella* were presented the same stimuli – one 2-minute scan and fifteen looming stimuli. I predicted that the looming-sensitive TSDNs would spike in a consistently timed manner before calculated time to contact for a realistic *l/v* looming stimulus, where the realistic stimuli had ratios $\frac{.22\text{ mm}}{.11\text{ m/s}}$, $\frac{.86\text{ mm}}{.43\text{ m/s}}$, and $\frac{3.4\text{ mm}}{1.73\text{ m/s}}$. Recall that the numerator, *l*, is defined as the half-size of the object, so the stimuli were double these sizes. I found that the data support my hypothesis. For a realistic *l/v*, looming-sensitive TSDNs fired 21 ms before Tc. This is the average spiketime, or time before Tc that a neuron fires, for all ten subjects. Because outliers can severely impact the mean spiketime of a series of spikes for a given looming stimulus, I calculated the median spiketime for every loom for every dragonfly. Presumably, those medians would not be outliers themselves, so I took the mean of those medians for the benefit of being able to calculate a standard deviation. Outside of the realistic *l/v* value, the standard deviation increased dramatically. Figure 8 shows the aggregated data from all ten dragonflies. Each

data point is the mean of the medians from all ten subjects. Because of the nature of the *l/v* values of the looming stimuli that I presented, there is more raw data for the moderate *l/v* looms than for the extreme ones. One can note from Figure 8 that several of the means or their standard deviations fell after Tc, which were represented by a positive value on the y-axis. A biological signal would not be helpful if it were received after the entire event has concluded, so this information tells a lot about the circumstances in which the TSDNs are useful. In Figure 8, I included the medians as well as the means to provide legitimacy for subsequent figures where I only use medians. For all the groups of looms with equal *l/v* values, the difference between the median and mean was less than 40% of one standard deviation of the mean, and seven of the nine different *l/v* groups had discrepancies below 20% of one standard deviation of the mean.

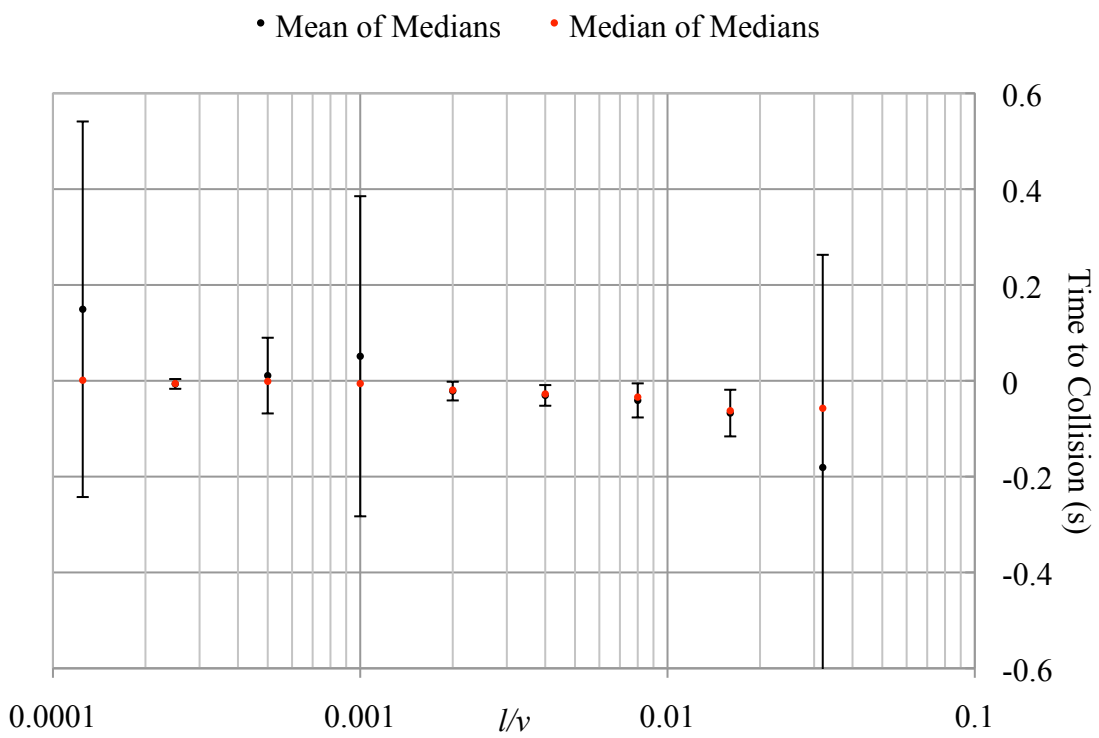

Figure 8. **Means of and medians of medians versus Tc.** This figure plots the *l/v* of the looming stimuli against the mean and median time to collision (Tc) for all data collected. Each subsequent *l/v* value is double the smaller one, but the x-axis is plotted on a logarithmic scale, deceptively giving the appearance of equal steps. The mean and medians are consistently close enough and within a fraction of a standard deviation of the mean that the usage of either metric is reasonable.

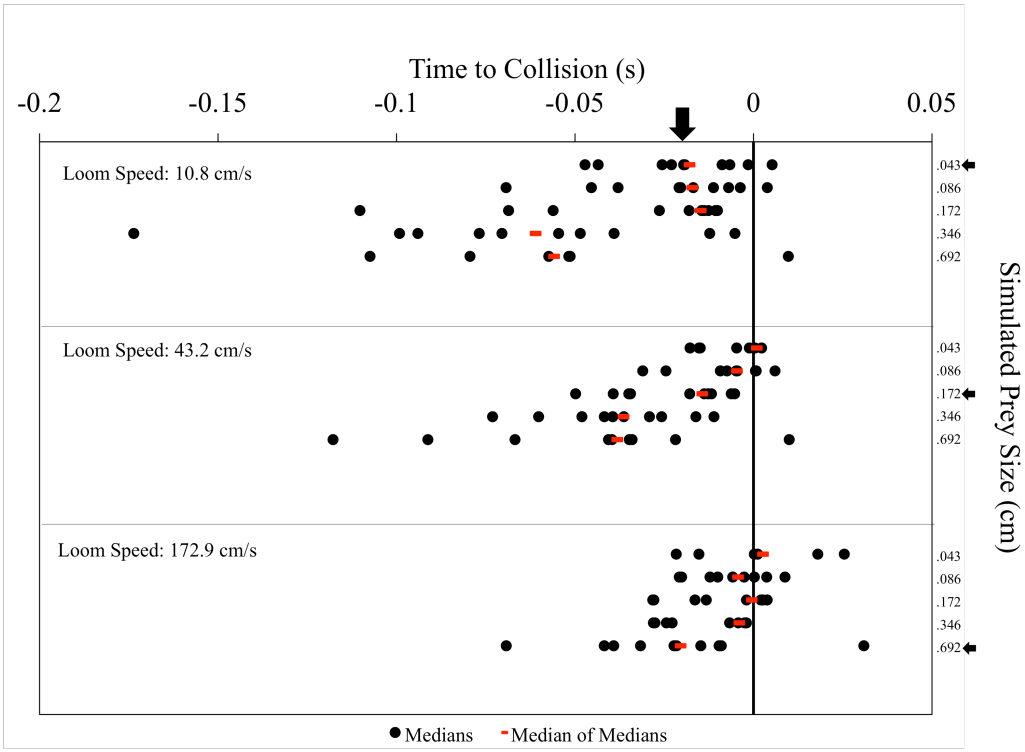

Figure 9. **Aggregate median of median spiketimes.** Each row of black dots is a single looming stimulus, and each black dot is the median spiketime for that loom for a single dragonfly. The red stripes are the medians of those daily medians. The 15 looming stimuli are broken into groups of three different speeds, and within those, each of the five different stimulus sizes at z = 0. The small black arrows point to the realistic *l/v* looms, and the larger downward-pointing arrow directs toward the the median spiketime for all of the realistic *l/v* data, represented by the red dot at *l/v* = 0.002 in Figure 8.

The same aggregate data is shown in Figure 9, but more subject-to-subject detail is provided. Whereas Figure 8 includes means, Figure 9 shows only the median spiketime of each dragonfly for each looming stimulus. This figure provides a visualization of the distribution of spikes for each animal. The red stripes are the medians of the median spiketimes – essentially an overall average spiketime before Tc for each loom – comparable to the red dots in Figure 8. Some of the looming stimuli are missing values here, which can be seen by the number of dots in each row. There are two reasons for this. The first is an artifact from the number of repetitive *l/v* values. There were three realistic *l/v* looming stimuli, but only one instance of each of the two smallest and largest *l/v* values, as can be seen in Figure 7. The second reason is that some of the more extreme

l/v looms did not elicit any spikes at all, which is an important conceptual finding when trying to implicate the TSDNs in any biological role.

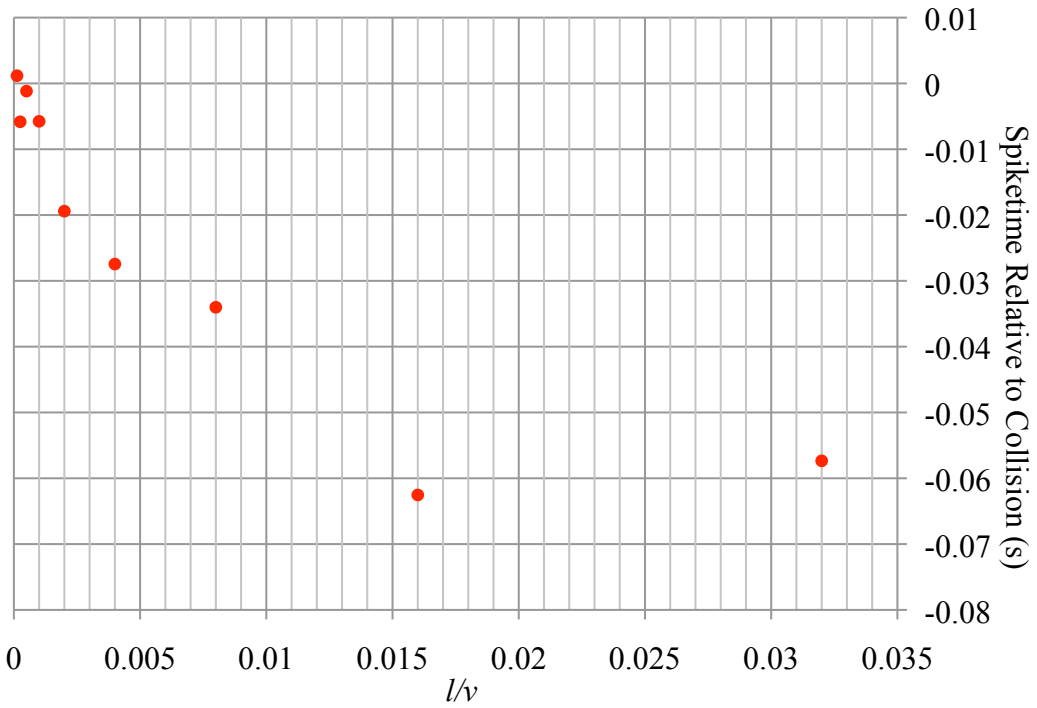

Figure 10. **Spiketimes relative to collision versus *l/v*.** It appears that as *l/v* increases, the TSDNs fire earlier, until some threshold when *l/v* no longer affects spiketime. Total aggregate medians of medians are shown. That is, for a single *l/v*, all collected data is compounded into one point. It is unclear if the relationship between spiketime before Tc and *l/v* follows a linear or logarithmic trend. Notation in previous figures remains the same – spiketime equal to 0 is Tc, and negative numbers on the y-axis are time before Tc. Data points are clustered toward the left side because *l/v* values were manipulated with a multiplier rather than linearly, and the x-axis is shown on a linear scale.

There were two trends in the relationship between response time and looming stimulus parameters. Generally, faster stimuli (descending in Figure 9) elicited spikes later in the course of the loom, while larger stimuli (descending within each stimulus speed in Figure 9) did the opposite. Both of trends are intuitive to us; it takes longer to notice a smaller object than a larger one, and we notice a slower object with more time before Tc than a faster object. So, both *l* and *v* each follow a general trend – both an increase in the former and a decrease in the latter will decrease the spike latency before Tc. Figure 10 shows the relationship between spiketimes before Tc and *l/v* – as a ratio

instead of individually – that was shown in Figure 8 as well. However, Figure 10 is zoomed in and distracting means and error bars have been omitted. It is now possible to see the trend, whereas it is exceedingly difficult to do so for the red dots in Figure 8. As *l/v* increases, the TSDN spike latency decreases, however, the exact nature of this relationship is not entirely clear. From Figure 10, it may appear that this trend is true until a certain point, after which the large *l/v* has no effect on when the TSDNs spike. Such a trend may be categorized as logarithmic. This may be deceiving though, as an especially large *l/v* may confound the data, especially because it is not a value of *l/v* that the dragonfly would encounter in nature. In the data with the greatest signal-to-noise ratio, the DIT3 did not spike at all during the presentation of the *l/v* = 0.032 stimulus. So, it may be that this relationship is linear rather than logarithmic.

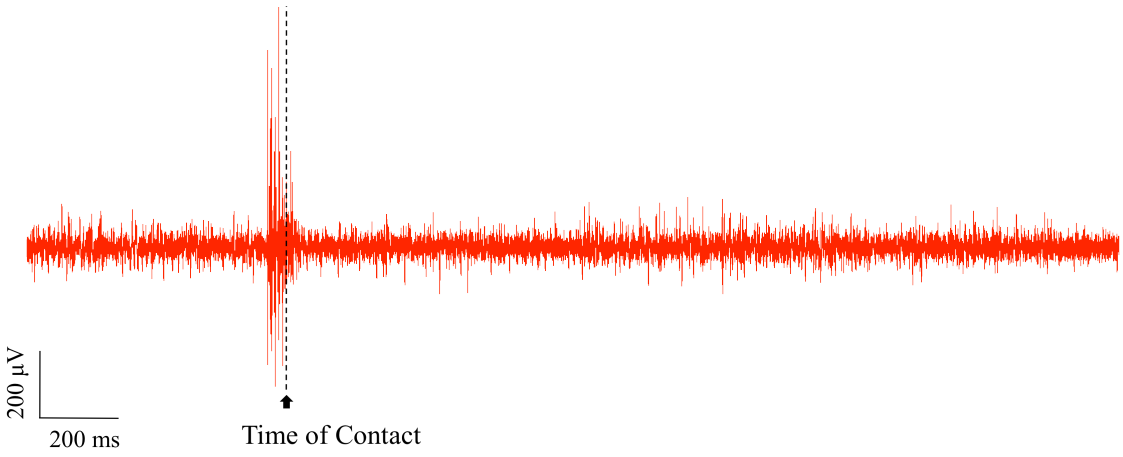

Figure 11. **Example trace.** This is one trace resulting from the *l* = 0.086 cm, *v* = 43.22 cm/s looming stimulus. The entire trace has duration of 2605 ms, but the actual stimulus was only projected for 1.16 s. The stimulus presentation ended briefly before Tc, and the three DIT3 spikes are immediately before Tc. Note that the *l* value is half of the stimulus size, as written in Figure 9, because *l* represents the radius of the simulated prey.

All neural recordings had the same duration, despite actual stimulus presentation time ranging from 0.15 s to 2.51 s. In Figure 11, the resulting neural trace from the medium speed, medium size (realistic *l/v*) is shown. Using the scanning stimulus, I

determined that I was recording from DIT3, one of the looming-sensitive TSDNs. DataView, the spike sorting software, determined that the DIT3 fired three times, which can be seen in Figure 11 immediately prior to Tc. Figure 12 is the output of the MATLAB script whose purpose is to show where on the screen the scanning stimulus was when the TSDN being recorded was spiking. This is the same data set which is shown in Figure 11. It is important to note how some directions elicit few or no spikes from DIT3 at all. However, it was the pattern of spikes from all eight directions of motion tested that enabled me to determine that I was recording from DIT3.

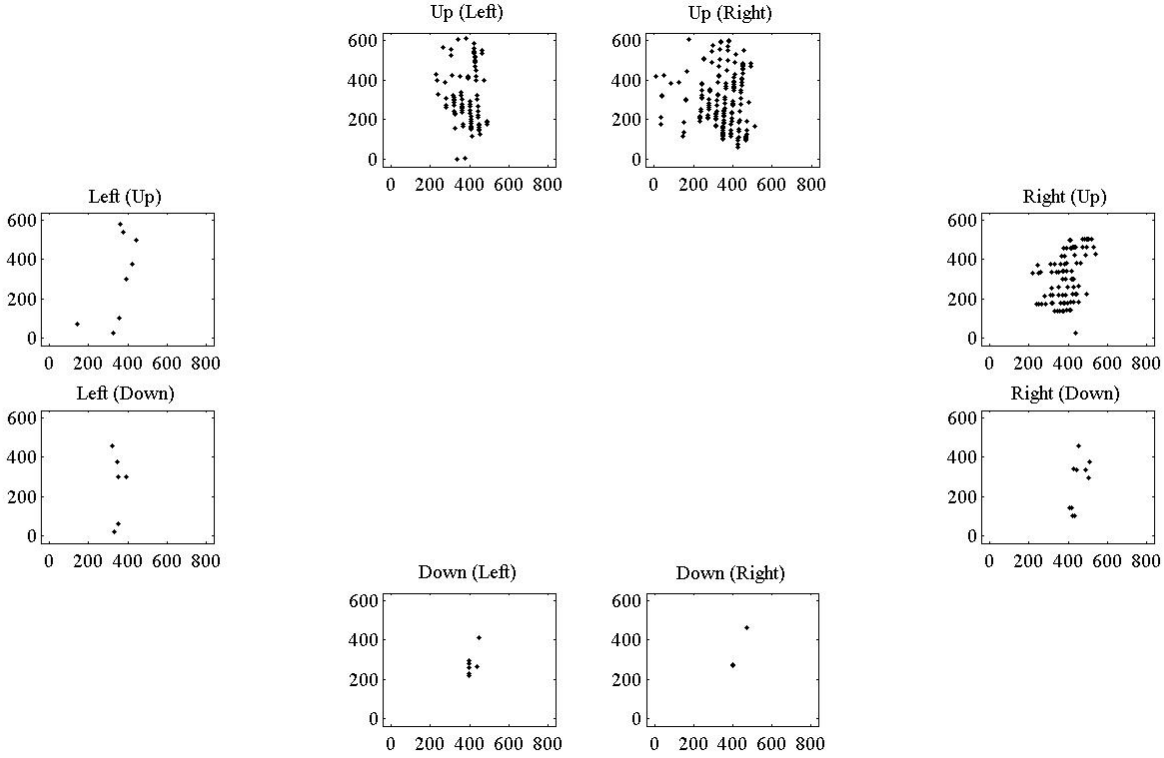

Figure 12. **Scanning stimulus spike locations**. Eight individual boxes (subplots) represent the eight directions the scanning stimulus moved. Each of the eight directions of the scan had a dominant and secondary direction of motion, just as each subplot is closer to some multiple of 90˚ – the dominant direction. Dominant direction is written above each plot (secondary direction in parenthesis). All axes are labeled with pixels on the 600x800 screen. Each black dot is where the stimulus was on the screen when the neuron fired, and the direction of motion of the stimulus is given by where the subplot is in relation to the center of the figure. No latency was accounted for in these spiking locations, which means that the stimulus location at the time of firing is shown, rather than the location that elicited the firing in the first place. For some of the subplots, the motion of the stimulus can be seen based on high frequency spikes. In these cases, the direction of motion follows a line that connects these black dots.

Discussion

Looming-sensitive TSDNs fired at a consistent time before calculated time-to-contact (Tc) for a time course of expansion (*l/v*) that the dragonflies would experience in nature. However, as can be seen in Figure 8, the standard deviation of the mean of the aggregate data for a realistic *l/v* was as large as the mean itself. This poses a problem with the hypothesis that TSDNs anticipate the approaching object, because statistically, over 15% of the daily spiketime medians came after Tc. A large component of this problem was the lack of electrophysiological data with a high signal-to-noise ratio. There was only one recording in which I was able to use DataView to categorize the spikes because the other data had too much noise. For a set of data with too much noise, I had to use a spike discriminator tool in LabChart and manually create spike voltage and frequency thresholds to assign which spikes were the TSDNs. The problem with this method is that it creates false positives – spikes register in my data set when a non-TSDN was firing. Further research will have to address this simply by collecting more, clean, sortable data. Of the several types of electrodes tested, glass microelectrodes were the best suited for extracellular, single-unit recordings. Recordings with high signal-to-noise ratios are achieved with careful analysis of the cross-sectional diagrams of the Anisoptera family of interest, and subsequent precise placement of the glass microelectrode.

These traces were noisy because the microelectrode was too far from the TSDNs of interest. This raises the issue of what the role is of these non-TSDNs that entered the data set as false positives. It is evident from the looming stimuli that they fire near Tc, so it is possible that they play a similar role as the TSDNs. As an example, one of these neurons may be visible in Figure 11 as the smaller spikes that are overshadowed by the

TSDNs prior to Tc. The neuron fires a few times before and after Tc, does not fire during a scanning stimulus, and is descending, but that is the limit of our knowledge of this cell. There are several possibilities for these neurons' role, but these results hint at the presence of other, non-TSDN, looming-sensitive neurons. There is no reason for there to only be two looming-sensitive neurons that are upstream of flight circuitry, but finding other ones in a sea of descending axons is a daunting task. If they do exist, they are probably not as important in flight behavior as the TSDNs because they are small, and therefore conduct more slowly. On the contrary, they may be part of circuitry that descends more directly from the retina to the thorax, saving time and spiking consistently with the TSDNs upon the presentation of a looming stimulus.

Fast-conducting neurons such as the locust DCMD are certainly crucial evolutionarily. The results show that the two TSDNs and the DCMD both respond to looming objects, but the way that they control their downstream post-synaptic neurons is different. The DCMD has a baseline firing rate and increases its spike frequency dramatically during the presentation of a looming stimulus (Gabbiani et al. 1999), whereas the data in the current study show that TSDNs spike just a few times, and this is probably sufficient in flight to control wing alterations. Moreover, the DCMD is a collision-avoidance neuron (Gray et al. 2001; Santer et al. 2006). The current study does not eliminate the possibility that the TSDNs are collision-avoidance neurons, but it does give support to the hypothesis that they have a role in the collision-seeking mechanisms of prey capture. Additional research will have to test this hypothesis further. This may be possible in future experimentation by recording from the TSDNs during actual prey capture. This is not yet completely feasible with today's technology, but when it is, we

will be able to test the TSDN response during prey capture, as well as during predation on dragonflies to fully test the neurons' capabilities and similarities to the DCMD.

From Figure 2, it is clear that most of the TSDNs lie on or near the dorsal surface of the ventral nerve cord. Traditional methods of accessing the nerve cord have been done so ventrally so that there is minimal invasion of other organs. However, this requires probing through the entire cord to reach the TSDNs of interest. If there were easy access to the nerve cord, it should follow that the easiest access to the TSDNs would be dorsally. So, I initially attempted this novel approach. It had promise because the dragonfly could be mounted right-side up and the TSDNs would lie at the start of the electrode's path in the nerve cord. For this dissection, I had to cut through cuticle, move the esophagus, and work around two airbags that press up against each other immediately dorsal to the nerve cord. I initially tried several different electrode types, including tungsten microelectrodes, silver, and glass suction electrodes. However, no combination of electrode and dorsal approach produced data. It is unclear exactly which factor or factors made this method unusable, but eventually I reverted to the traditional ventral approach and used a glass microelectrode.

Unfortunately, problems in obtaining clean recordings took so much time that I was unable to account for other confounding variables when collecting usable data. An example of this was the temperature. Olberg et al. (2007) discuss the shorter visual latencies in the sun's warmth than in a dark, room temperature laboratory. Therefore, spiketimes before Tc should be even earlier for a dragonfly in a natural setting. Dragonflies extend their legs 20 ms before prey capture (Worthington, unpublished), and I found that for a realistic *l/v*, looming-sensitive TSDNs fire about 20 ms before Tc. If

both of these are true, then those TSDNs cannot be upstream of leg control muscle circuitry – there is not enough time. However, this may be possible if TSDNs fire earlier at higher body temperatures. We cannot rule out the possibility of a connected circuit until the TSDN response is recorded in a natural setting, which, at a minimum, must be warm and have plenty of UV and short-wavelength visible light. Future studies may include performing a similar experiment but in the animal's natural habitat.

Another limitation of the current study is that we know dragonflies are able to determine depth because they ascend to capture a small, slow-moving fly, but not a large, fast-moving bird (Olberg et al. 2000). In this regard, it is highly likely that the TSDN response to looming stimuli on a 2D screen does not contain all the information that it otherwise would in a 3D setting. To account for this, concurrent research (Zinman et al., accepted) is being developed to create a 3D flight simulator. The simulator uses a similar glass bead to what has been used in past studies (Olberg et al. 2005), but instead of being manipulated manually on a thread, its position can be shifted in all three dimensions at a realistic speed and acceleration for typical dragonfly prey. With this technology, similar scanning and looming stimuli can be presented with varying parameters, and in addition, different size beads can be used. In effect, it will be able to produce all of the motions that I developed and more, with the added benefit of the prey being a real, 3D object.

Future studies may investigate how TSDNs respond to stimuli that simulate predators. DMT1 responds to moving objects behind the dragonfly (Olberg 1986), so it is possible that the TSDN plays a role in predator evasion. However, it does not appear to be looming-sensitive, which does not support this hypothesis. Olberg et al. (2000) show that close-by prey have a notably different angular velocity than potential predators that

are far away. The difference in angular velocity may be accounted for in the TSDN spike patterns, and so the dragonfly would be able to evade the predator long before any approaching movement. This can be tested by analyzing the TSDN response to far, large, fast-moving objects. An *l/v* value could be used that emulates a flying bird, along with one that is equivalent to a close-by food item, but scaled farther, larger, and faster, in order to relate back to the current study.

The TSDNs, especially those that are looming-sensitive, are imperative in the dragonfly's ability to catch prey, but they are only one part of a visual system that accounts for much of its nervous system. The dragonflies are masters of evasion and capture, and have perfected both of those techniques over hundreds of millions of years. The neural circuitry is remarkably simple for their complex behavior, and there is a lot that we can learn from both their behavior and from the nervous system controlling it.

References

Baird JM, May ML (1997) Foraging behavior of *Pachydiplax longipennis* (Odonata: Libellulidae). J Insect Behav 10:655-678

Collett TS, Land MF (1978) How hoverflies compute interception courses. J Comp Physiol 125:191-204

Corbet PS (1999) Dragonflies: behavior and ecology of Odonata. Cornell University Press, Ithaca, NY

Frye MA, Olberg RM (1995) Visual receptive field properties of feature detecting neurons in the dragonfly. J Comp Physiol A 177:569-576

Gabbiani G, Krapp HG, Laurent G (1999) Computation of object approach by a wide-field, motion-sensitive neuron. J Neurosci 19:1122-1141

Geurten, BRH, Nordström K, Sprayberry JDH, Bolzon DM, O'Carroll DC (2007) Neural mechanisms underlying target detection in a dragonfly centrifugal neuron. J Exp Bio 210:3277-3284

Gray JR, Lee JK, Robertson RM (2001) Activity of descending contralateral movement detector neurons and collision avoidance behaviour in response to head-on visual stimuli in locusts. J Comp Physiol A 187:115-129

Needham JG, Westfall Jr. MJ, May ML (2000) Dragonflies of North America. Scientific Publishers, Gainesville, FL

Nikula B, Loose JL, Burne MR (2003) A field guide to the dragonflies and damselflies of Massachusetts. Mass. Division of Fisheries and Wildlife, Westborough, MA

Olberg RM (1983) Identified interneurons steer flight in the dragonfly. Soc Neurosci Abstr 9:326

Olberg RM (1986) Identified target-selective visual interneurons descending from the dragonfly brain. J Comp Physiol A 159:827-840

Olberg RM, Seaman RC, Coats MI, Henry AF (2007) Eye movements and target fixation during dragonfly prey-interception flights. J Comp Physiol A 193:685-693

Olberg RM, Worthington AH, Venator KR (2000) Prey pursuit and interception in dragonflies. J Comp Physiol 186:155-162

Ruck P (1961) Electrophysiology of the insect dorsal ocellus III. Responses to flickering light of the dragonfly ocellus. J Gen Physiol 44:641-657

Rüppell G (1989) Kinematic analysis of symmetrical flight manoeuvres of Odonata. J Exp Bio 144:13-42

Santer RD, Rind FC, Stafford R, Simmons PJ (2006) Role of an identified looming-sensitive neuron in triggering a flying locust's escape. J Neurophysiol 95:3391-3400

Sherk TE (1978) Development of the compound eyes of dragonflies (Odonata) III. Adult compound eyes. J Exp Zool 203:61-80

Silsby J (2001) Dragonflies of the world. Smithsonian Institution Press, Washington, DC

Wakeling JM, Ellington CP (1997) Dragonfly flight: velocities, accelerations and kinematics of flapping flight. J Exp Bio 200:557-582.

Wiederman SD, O'Carroll DC (2011) Discrimination of features in natural scenes by a dragonfly neuron. J Neurosci 31:7141-7144

Zinman AR, Balter ML, Olberg RM, Ramasubramanian A, Hodgson D (2012) Design, construction, and testing of a flying prey simulator. 5th Annual Dynamic Systems and Control Conference (in press)

Appendix

```
clear
% Takes the name of the spiketimes file. This file should have times in seconds,
% each column is a different neuron, each row is a different spike.
sp = input('enter the spiketime file name ','s');
spt = [sp '.txt']; % Adds '.txt' to the end of the inputted spiketimes file name.
sptimes = dlmread(spt); % Reads first line in the spiketimes file.
%first = input('enter number of first block of the scan ');
%last = first + 7;
%Creates a vector of the block start times during the scan:
%blocks = [15*(first-1):15:15*(first+7)];
% Splits 'blocks' into matrix from 0-120 in increments of
blocks = (0:15:120); % 15 (seconds) for 8 blocks total.
blocks = blocks'; % Converts blocks to a column
% Designate which column in sptimes to use - which neuron are we plotting?:
unit = input('enter unit number ');

for i=1:8 %create a bundle of spiketimes in each block and make the times start = 0
    block(i).times = sptimes( sptimes(:,unit) > blocks(i) & ...
        sptimes(:,unit) < blocks(i+1) , unit); % Fixed for logical indexing.
    % Finds the times for the unit in the time range set by the intervals in blocks
    % Assigns it to its own variable.
    % Brings the spiketime down so that it is between 0 and 15 (seconds).
    block(i).times = block(i).times - blocks(i);
end

path = dlmread('scanpath.txt','%t');
for i=1:8 %find coordinates indices corresponding to each spiketime in block
    spikeindices(i).log = dsearchn( path(:,1), block(i).times );
    locations(i).log = path(spikeindices(i).log,2*i:(2*i)+1);
    locations(i).log(:,2) = 600-locations(i).log(:,2); %flips y values
end
figure

for i = 1
    subplot(4,4,8), scatter(locations(i).log(:,1),locations(i).log(:,2),'.','k')
    hold on
end
axis equal
xlim([-40 840])
ylim([-40 640])
box on
title('Right (Up)')

for i = 2
    subplot(4,4,5), scatter(locations(i).log(:,1),locations(i).log(:,2),'.','k')
    hold on
end
axis equal
xlim([-40 840])
ylim([-40 640])
box on
title('Left (Up)')

for i = 3
```

```
    subplot(4,4,3), scatter(locations(i).log(:,1),locations(i).log(:,2),'.','k')
    hold on
end
axis equal
xlim([-40 840])
ylim([-40 640])
box on
title('Up (Right)')

for i = 4
    subplot(4,4,15), scatter(locations(i).log(:,1),locations(i).log(:,2),'.','k')
    hold on
end
axis equal
xlim([-40 840])
ylim([-40 640])
box on
title('Down (Right)')

for i = 5
    subplot(4,4,12), scatter(locations(i).log(:,1),locations(i).log(:,2),'.','k')
    hold on
end
axis equal
xlim([-40 840])
ylim([-40 640])
box on
title('Right (Down)')

for i = 6
    subplot(4,4,9), scatter(locations(i).log(:,1),locations(i).log(:,2),'.','k')
    hold on
end
axis equal
xlim([-40 840])
ylim([-40 640])
box on
title('Left (Down)')

for i = 7
    subplot(4,4,2), scatter(locations(i).log(:,1),locations(i).log(:,2),'.','k')
    hold on
end
axis equal
xlim([-40 840])
ylim([-40 640])
box on
title('Up (Left)')

for i = 8
    subplot(4,4,14), scatter(locations(i).log(:,1),locations(i).log(:,2),'.','k')
    hold on
end
axis equal
xlim([-40 840])
ylim([-40 640])
```

```
box on
title('Down (Left)')

bf=int2str(1); %turn the block number into a string
bl=int2str(8);
un=int2str(unit);
gtext([sp   ' unit ' un ': Blocks ' bf ' to ' bl])
```

Published with MATLAB® 7.11

Figure 13. **MATLAB scan code**. This code was written in MATLAB, originally by Robert Olberg and modified by me to apply to the current study. It inputs a file that gives the location and time of the scanning stimulus at very short intervals, and a file that lists the times when the units fired. With these pieces of information, it outputs what can be seen in Figure 12 – the locations on the screen when the neuron fired.

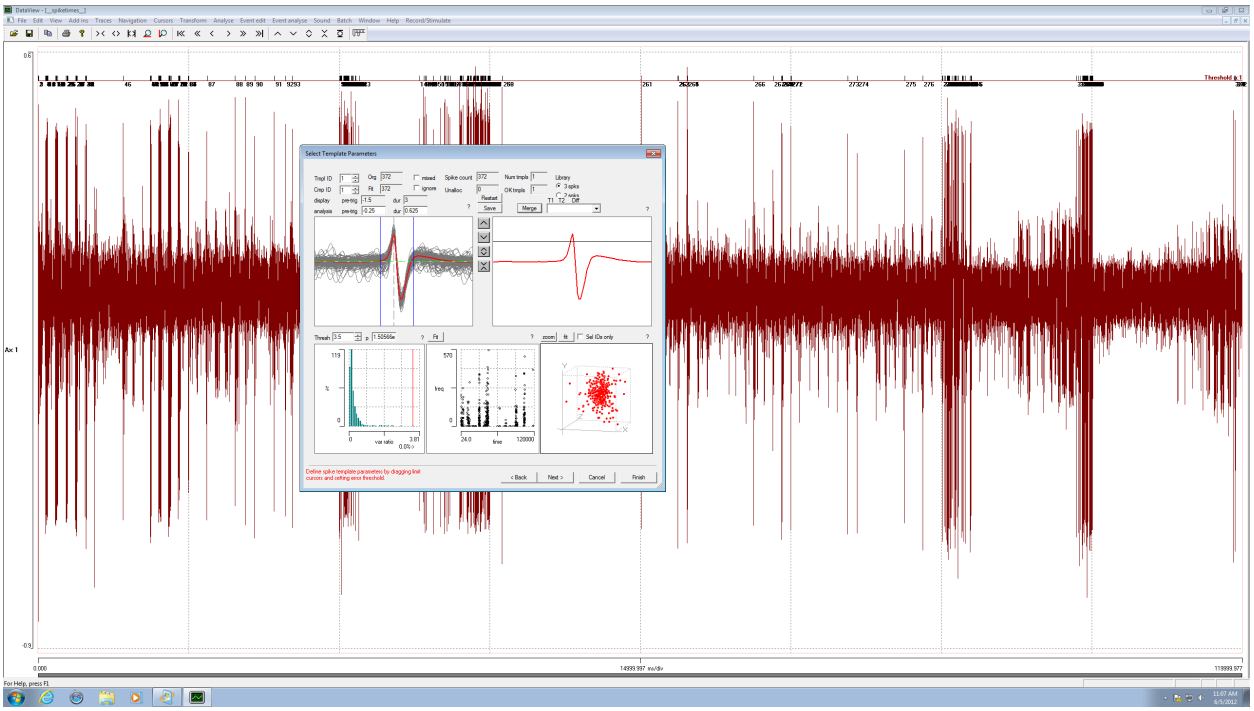

Figure 14. **DataView screenshot**. This is a snapshot of the DataView software used to determine at what precise times each neuron is firing. In the background is the entire trace from the 2-minute scanning stimulus. In the foreground is the spike sorting wizard, which allows the user to set time and instantaneous frequency thresholds, group and split spike templates based on waveform, and assign or unassign individual spikes to those templates.